A Nonparametric CUSUM Chart For Monitoring Multivariate Serially Correlated Processes

Li Xue[1] and Peihua Qiu[2]

[1]School of Information Management, Zhengzhou University of Aeronautics, Zhengzhou,450046, China

[2]Department of Biostatistics, University of Florida, Gainesville, FL 32610, USA

Abstract

In applications, most processes for quality control and management are multivariate. Thus, multivariate statistical process control (MSPC) is an important research problem and has been discussed extensively in the literature. Early MSPC research is based on the assumptions that process observations at different time points are independent and they have a parametric distribution (e.g., Gaussian) when the process is in-control (IC). Recent MSPC research has lifted the "parametric distribution" assumption, and some nonparametric MSPC charts have been developed. These nonparametric MSPC charts, however, often requires the "independent process observations" assumption, which is rarely valid in practice because serial data correlation is common in a time series data. In the literature, it has been well demonstrated that a control chart who ignores serial data correlation would be unreliable to use when such data correlation exists. So far, we have not found any existing nonparametric MSPC charts that can accommodate serial data correlation properly. In this paper, we suggest a flexible nonparametric MSPC chart which can accommodate stationary serial data correlation properly. Numerical studies show that it performs well in different cases.

Key Words: Data correlation; Decorrelation; Moment estimation; Nonparametric charts; Stationary data correlation; Statistical process control.

1 Introduction

Statistical process control provides a powerful tool for quality control and monitoring of longitudinal processes (Hawkins and Olwell 1998, Montgomery 2012, Qiu 2014). In practice, to measure the quality of a process, multiple quality variables are usually needed. So, multivariate statistical process control (MSPC) is an important research problem. This paper aims to develop a general multivariate control chart that would be reliable to use when process observations are serially correlated and process distribution is nonparametric.

Because of its importance, MSPC has been discussed extensively in the literature. Early MSPC methods require the assumptions that multivariate process observations are independent at different time points and the in-control (IC) process distribution is multivariate normal or another parametric distribution (e.g., Crosier 1988, Hawkins 1991, Healy 1987, Lowry et al. 1992, Tracy et al. 1992). In practice, the assumed parametric distribution would be rarely valid and consequently the above-mentioned MSPC charts would be unreliable to use. To overcome that limitation, more recent MSPC research has focused on developing nonparametric MSPC charts that does not require the parametric distribution assumption. See, for instance, Boone and Chakraborti (2012), Chen et al. (2016), Holland and Hawkins (2014), Liu (1995), Qiu (2008, 2018, 2020), Qiu and Hawkins (2001, 2003), Zou and Tsung (2011), Zou et al. (2012), and the references cited therein. These methods, however, all assume that process observations are independent at different time points. In applications, serial data correlation is common in time series data. Thus, that assumption would be rarely valid. In the literature, it has been well demonstrated that control charts could be unreliable to use if they ignore serial data correlation in the observed data (e.g., Apley and Lee 2008, Li and Qiu 2020, Qiu et al. 2020, Runger 2002). Therefore, it is critically important to develop nonparametric MSPC charts that can accommodate serial data correlation. So far, we could not find such nonparametric MSPC charts in the literature yet. This paper aims to fill the gap by proposing a general multivariate CUSUM chart for online process monitoring, which can accommodate stationary serial data correlation without imposing any parametric form on the IC process distribution. This chart only requires a small-to-moderate IC dataset. Thus, it is convenient to use in applications. Numerical studies show that it works well in various different cases considered.

The remaining parts of the article is organized as follows. Our proposed nonparametric MSPC chart is described in detail in Section 2. Its numerical performance is evaluated in Section 3 by several simulation examples. Then, the chart is applied to a real-data example about a semiconductor manufacturing process in Section 4. Several remarks conclude the paper in Section 5.

2 Nonparametric MSPC Chart For Monitoring Serially Correlated Data

Our proposed chart focuses mainly on online monitoring of p-dimensional processes, where $p > 0$ is an interger. Let the sequence of process observations under sequential monitoring be $\{\mathbf{X}_n = (X_{n1}, X_{n2}, \ldots, X_{np})', n \geq 1\}$. One assumption needed by our proposed chart is that the serial data correlation in the observed data is stationary when the process is IC, which implies that

the covariance matrix $\boldsymbol{\gamma}(s) = \text{Cov}(\boldsymbol{X}_i, \boldsymbol{X}_{i+s})$, for any i, depends only on s in such cases. This assumption should be reasonable because it is believed that the IC process distribution, including the IC serial data correlation, does not change over time in many applications, including the production lines in the manufacturing industry. Regarding the serial data correlation of an IC process, it is also assumed that there is an integer $w \geq 1$ such that $\boldsymbol{\gamma}(s) = \mathbf{0}$ when $s > w$. This assumption implies that the correlation between two observations would disappear if the related observation times are far away, which should be (approximately) true in many applications. For online process monitoring, the IC process distribution is assumed to be unknown and nonparametric. Instead, we assume there is a small-to-moderate set of IC observations $\boldsymbol{X}_{IC} = \{\boldsymbol{X}_{-m_0+1}, \boldsymbol{X}_{-m+2}, \ldots, \boldsymbol{X}_0\}$ with the sample size of m, collected before online process monitoring. Such IC data are often available in manufacturing applications, after Phase-I process monitoring. See a related discussion in Section 1.3 of Qiu (2014).

Our proposed chart is a self-starting nonparametric CUSUM chart. As a self-starting chart, certain IC parameters used in the chart need to be estimated initially from the IC data and then the initial estimates can be constantly updated during online process monitoring (cf., Hawkins 1987). To this end, the IC mean $\boldsymbol{\mu}$ and the IC variance/covariance matrices $\{\boldsymbol{\gamma}(s), 0 \leq s \leq w\}$ are first estimated from the IC data $\boldsymbol{X}_{IC}$ as follows: for any $0 \leq s \leq w$, let

$$\begin{aligned} \widehat{\boldsymbol{\mu}}^{(0)} &= \frac{1}{m_0} \sum_{i=-m_0+1}^{0} \boldsymbol{X}_i, \\ \widehat{\boldsymbol{\gamma}}^{(0)}(s) &= \frac{1}{m_0 - s} \sum_{i=-m_0+1}^{-s} \left(\boldsymbol{X}_{i+s} - \widehat{\boldsymbol{\mu}}^{(0)}\right)\left(\boldsymbol{X}_i - \widehat{\boldsymbol{\mu}}^{(0)}\right)'. \end{aligned}$$

Then, the IC data can be de-correlated recursively by the following algorithm that is based on the Cholesky decomposition of the covariance matrices:

Recursive Algorithm for Decorrelating the Multivariate IC Data

- When $i = -m_0 + 1$, the de-correlated and standardized observation is defined to be $\boldsymbol{X}_i^* = [\widehat{\boldsymbol{\gamma}}^{(0)}(0)]^{-1/2}(\boldsymbol{X}_i - \widehat{\boldsymbol{\mu}}^{(0)})$, and an auxiliary parameter b is set to be 1.
- For $i > -m_0+1$, the estimated covariance matrix of $(\boldsymbol{X}'_{i-b+1}, \boldsymbol{X}'_{i-b+2}, \ldots, \boldsymbol{X}'_i)'$ can be defined to be

$$\widehat{\boldsymbol{\Sigma}}_{i,i} = \begin{pmatrix} \widehat{\boldsymbol{\gamma}}^{(0)}(0) & \cdots & \widehat{\boldsymbol{\gamma}}^{(0)}(b) \\ \vdots & \ddots & \vdots \\ [\widehat{\boldsymbol{\gamma}}^{(0)}(b)]' & \cdots & \widehat{\boldsymbol{\gamma}}^{(0)}(0) \end{pmatrix} = \begin{pmatrix} \widehat{\boldsymbol{\Sigma}}_{i-1,i-1} & \widehat{\boldsymbol{\sigma}}_{i-1} \\ [\widehat{\boldsymbol{\sigma}}_{i-1}]' & \widehat{\boldsymbol{\gamma}}^{(0)}(0) \end{pmatrix},$$

where $\widehat{\boldsymbol{\sigma}}_{i-1} = ([\widehat{\boldsymbol{\gamma}}^{(0)}(b)]', \ldots, [\widehat{\boldsymbol{\gamma}}^{(0)}(1)]')'$. Then, the ith de-correlated and standardized observation is defined to be

$$\boldsymbol{X}_i^* = \widehat{\boldsymbol{D}}_i^{-1/2} \left\{ \boldsymbol{X}_i - \widehat{\boldsymbol{\mu}}^{(0)} - \widehat{\boldsymbol{\sigma}}_{i-1}' \widehat{\boldsymbol{\Sigma}}_{i-1,i-1}^{-1} \widehat{\boldsymbol{e}}_{i-1} \right\},$$

where $\widehat{\boldsymbol{D}}_i = \widehat{\boldsymbol{\gamma}}^{(0)}(0) - \widehat{\boldsymbol{\sigma}}_{i-1}' \widehat{\boldsymbol{\Sigma}}_{i-1,i-1}^{-1} \widehat{\boldsymbol{\sigma}}_{i-1}$, and $\widehat{\boldsymbol{e}}_{i-1} = ((\boldsymbol{X}_{i-b} - \widehat{\boldsymbol{\mu}}^{(0)})', \ldots, (\boldsymbol{X}_{i-1} - \widehat{\boldsymbol{\mu}}^{(0)})')'$. Let $b = \min(b+1, w)$ and $i = i+1$. Repeat this step until $i > 0$.

In the above decorrelation algorithm, the following Cholesky decomposition has been used. Let $\boldsymbol{\Sigma}_{i,i}$ be the covariance matrix of $\boldsymbol{e}_i = ((\boldsymbol{X}_{i-b+1} - \boldsymbol{\mu}^{(0)})', (\boldsymbol{X}_{i-b+2} - \boldsymbol{\mu}^{(0)})', \ldots, (\boldsymbol{X}_i - \boldsymbol{\mu}^{(0)})')'$. Then, $\boldsymbol{\Sigma}_{i,i}$ has the Cholesky decomposition: $L_i \boldsymbol{\Sigma}_{i,i} L_i' = U_i$, where $L_i = \begin{pmatrix} L_{i-1} & \boldsymbol{0} \\ -\boldsymbol{\sigma}_{i-1}' \boldsymbol{\Sigma}_{i-1,i-1}^{-1} & I_{p\times p} \end{pmatrix}$, $U_i = \mathrm{diag}(\boldsymbol{D}_{i-b+1}, \ldots, \boldsymbol{D}_i)$, and $\boldsymbol{D}_i = \boldsymbol{\gamma}^{(0)}(0) - \boldsymbol{\sigma}_{i-1}' \boldsymbol{\Sigma}_{i-1,i-1}^{-1} \boldsymbol{\sigma}_{i-1}$. Therefore, the covariance matrix of $U_i^{-1/2} L_i \boldsymbol{e}_i$ is the identity matrix, and $\boldsymbol{X}_i^*$ defined above is the vector of its last p elements, after $\boldsymbol{\mu}^{(0)}$ and $\boldsymbol{\gamma}^{(0)}(0)$ are replaced by their estimates and $\{\boldsymbol{D}_i\}$ are replaced by $\{\widehat{\boldsymbol{D}}_i\}$. Thus, if $\widehat{\boldsymbol{\mu}}^{(0)}$ and $\{\widehat{\boldsymbol{\gamma}}^{(0)}(s), 0 \le s \le w\}$ were the true IC process mean and variance/covariance matrices, then the de-correlated and standardized observations $\{\boldsymbol{X}_i^*, i = -m_0+1, \ldots, 0\}$ would be uncorrelated and each would have $\boldsymbol{0}$ mean and identity variance matrix. Because the sample size m_0 of the IC data could be small, $\widehat{\boldsymbol{\mu}}^{(0)}$ and $\{\widehat{\boldsymbol{\gamma}}^{(0)}(s), 0 \le s \le w\}$ may not be accurate estimates of the IC process mean and variance/covariance matrices. To overcome this limitation, a self-starting control chart is suggested below, in which the estimates of the IC process mean and variance/covariance matrices are constantly updated.

To online monitor the multivariate process observations $\{\boldsymbol{X}_n, n \ge 1\}$, at the current time point n, the estimates of the IC mean $\boldsymbol{\mu}$ and the IC variance/covariance matrices $\{\boldsymbol{\gamma}(s), 0 \le s \le w\}$ can be updated recursively as follows: for $n \ge 1$ and $0 \le s \le w$,

$$\widehat{\boldsymbol{\mu}}^{(n)} = \frac{1}{m_0+n} \boldsymbol{X}_n + \frac{m_0+n-1}{m_0+n} \widehat{\boldsymbol{\mu}}^{(n-1)}, \tag{1}$$

$$\widehat{\boldsymbol{\gamma}}^{(n)}(s) = \frac{1}{m_0+n-s} (\boldsymbol{X}_n - \widehat{\boldsymbol{\mu}}^{(n)})(\boldsymbol{X}_{n-s} - \widehat{\boldsymbol{\mu}}^{(n)}) + \frac{m_0+n-s-1}{m_0+n-s} \widehat{\boldsymbol{\gamma}}^{(n-1)}(s). \tag{2}$$

Next, we need to decorrelate and standardize the process observations $\{\boldsymbol{X}_n, n \ge 1\}$ properly so that a conventional control chart can be applied to them since the conventional control chart would not be appropriate to use if process observations are correlated. However, in cases when n is large, the computation involved in decorrelating $\boldsymbol{X}_n$ and its previous process observations could be quite intensive. To reduce computation, we suggesting making use of the restarting mechanism of a CUSUM chart that all previous observations up to the current time point n can be ignored in subsequent process monitoring if the observed data up to n suggest that a process distributional shift is unlikely. Based on the restarting mechanism of the CUSUM chart, Chatterjee and Qiu

(2009) defined the so-called spring length T_n which was the number of observation times between the current time point n and the last time point when the CUSUM charting statistic is zero. By this idea, at the current time point n, we only need to decorrelate $\boldsymbol{X}_n$ with the previous T_{n-1} observations for subsequent process monitoring. From our numerical experience, T_{n-1} is often a single digit integer number. Thus, it indeed can reduce computation in a substantial way. At the time n, data decorrelation between $\boldsymbol{X}_n$ and $\{\boldsymbol{X}_{n-T_{n-1}}, \ldots, \boldsymbol{X}_{n-1}\}$ can be achieved using a procedure similar to the one described above for decorrelating the IC data.

If the original observations $\boldsymbol{X}_1, \boldsymbol{X}_2, \ldots$ are normally distributed, then the decorrelated and standardized observations, denoted as ${\boldsymbol{X}_1}^*, {\boldsymbol{X}_2}^*, \ldots$, would be roughly i.i.d. and normally distributed as well. In such cases, the conventional multivariate charts, such as the conventional multivariate CUSUM and EWMA charts (e.g., Crosier 1988, Lowry et al. 1992) should be appropriate to use for monitoring the decorrelated and standardized observations. However, the IC process distribution could be substantially different from a normal distribution. In such cases, the distribution of the decorrelated and standardized observations could be substantially different from a normal distribution too. Consequently, the conventional charts would be unreliable and their results could be misleading in such cases (cf., the related discussion in Section 1). For this reason, we suggest using the multivariate nonparametric CUSUM chart that was originally discussed in Qiu (2008) for monitoring the decorrelated and standardized observations ${\boldsymbol{X}_1}^*, {\boldsymbol{X}_2}^*, \ldots$. Construction of this chart is described below.

Qiu (2008) sugegsted a general framework to construct a nonparametric control chart. By this framework, original quality variables can be categorized first. Then, the IC relationship among multiple categorized quality variables can be described by using a log-linear model. Based on the IC distribution described by this model, a nonparametric control chart can be constructed by comparing the observed count of the categorized quality variables in a given category with the corresponding expected count, which is similar to the idea of the Pearson's ch-square test (cf., Agresti 2013). By this framework to construct a nonparametric control chart, the decorrelated and standardized process observations $\boldsymbol{X}_n^* = (X_{n1}^*, X_{n2}^*, \ldots, X_{np}^*)'$ should be categorized as follows:

$$Y_{nj}^* = I(X_{nj}^* > m_j^*), \quad for \quad j = 1, 2, \ldots, p, \tag{3}$$

where m_j^* is the IC median of X_{nj}^*, for $j = 1, 2, \ldots, p$, and $I(u)$ is the indicator function that equals 0 and 1 when u is "false" and "true", respectively. Let $\boldsymbol{Y}_n^* = (Y_{n1}^*, Y_{n2}^*, \ldots, Y_{np}^*)'$. Then, $\boldsymbol{Y}_n^*$ is the categorized version of $\boldsymbol{X}_n^*$. When the process is IC, let

$$f_{j_1,\ldots,j_p}^{(0)} = P(Y_{n1}^* = j_1, \ldots, Y_{np}^* = j_p), \qquad \text{for } j_1, \ldots, j_p = 0, 1,$$

and $\boldsymbol{f}^{(0)}$ be a long vector with elements $\{f_{j_1,\ldots,j_p}^{(0)}, j_1, \ldots, j_p = 0, 1\}$. Then, the IC distribution

$\boldsymbol{f}^{(0)}$ can be estimated from the IC dataset, using the log-linear modeling approach that can be accomplished by using the R-function log-lin(). Let

$$g_{j_1,\ldots,j_p}(n) = I(Y^*_{n1} = j_1, \ldots, Y^*_{np} = j_p), \qquad \text{for } j_1, \ldots, j_p = 0, 1,$$

$\boldsymbol{g}(n)$ be the long vector with elements $\{g_{j_1,\ldots,j_p}(n), j_1, \ldots, j_p = 0, 1\}$ arranged in the same order as that in $\boldsymbol{f}^{(0)}$. Then, $g_{j_1,\ldots,j_p}(n)$ is the observed count of the $(j_1, \ldots, j_p)$ and $f^{(0)}_{j_1,\ldots,j_p}$ is the expected count. By combining the construction of a multivariate CUSUM chart (cf., Crosier 1988) and the Pearson's ch-square test, we consider the following CUSUM charting statistic:

$$C_n = (\boldsymbol{S}^{obs}_n - \boldsymbol{S}^{exp}_n)' \, [diag(\boldsymbol{S}^{exp}_n)]^{-1} \, (\boldsymbol{S}^{obs}_n - \boldsymbol{S}^{exp}_n), \tag{4}$$

where

$$\begin{cases} \boldsymbol{S}^{obs}_n = \boldsymbol{S}^{exp}_n = \boldsymbol{0}, & \text{if } D_n \le k, \\ \boldsymbol{S}^{obs}_n = (\boldsymbol{S}^{obs}_{n-1} + \boldsymbol{g}(n))(D_n - k)/D_n, & \text{if } D_n > k, \\ \boldsymbol{S}^{exp}_n = (\boldsymbol{S}^{exp}_{n-1} + \boldsymbol{f}^{(0)})(D_n - k)/D_n, & \text{if } D_n > k, \end{cases}$$

$$D_n = \left[(\boldsymbol{S}^{obs}_{n-1} - \boldsymbol{S}^{exp}_{n-1}) + (\boldsymbol{g}(n) - \boldsymbol{f}^{(0)}) \right]' \left[diag(\boldsymbol{S}^{obs}_{n-1} + \boldsymbol{f}^{(0)}) \right]^{-1} \left[(\boldsymbol{S}^{obs}_{n-1} - \boldsymbol{S}^{exp}_{n-1}) + (\boldsymbol{g}(n) - \boldsymbol{f}^{(0)}) \right],$$

$diag(\boldsymbol{a})$ denotes a diagonal matrix with the diagonal elements being those in $\boldsymbol{a}$, and k is an allowance parameter. Then, the chart gives a shift if

$$C_n > h, \tag{5}$$

where $h > 0$ is a control limit. In (4), $\boldsymbol{S}^{obs}_n$ is the vector of cumulative observed counts by the current time point n, and $\boldsymbol{S}^{exp}_n$ is the vector of cumulative expected counts. Thus, C_n measures the difference between the cumulative observed counts and the cumulative expected counts, while the re-starting mechanism of the CUSUM chart is maintained by using the allowance parameter k when defining $\boldsymbol{S}^{obs}_n$ and $\boldsymbol{S}^{exp}_n$.

In the data categorization process (cf., (3)), the IC medians $\{m^*_j, j = 1, 2, \ldots, p\}$ need to be obtained in advance. These parameters can be first estimated from the IC data by the sample medians, and then the estimates can be updated recursively at the current time point n if the CUSUM chart (4)-(5) confirms that the process is IC at n. More specifically, if the chart (4)-(5) does not give a signal at time n, then $\boldsymbol{X}^*_n$ can be combined with the previous IC dataset, and the sample medians could be updated recursively to improve their accuracy in estimating the corresponding IC medians $\{m^*_j, j = 1, 2, \ldots, p\}$. Let the sample medians from the decorrelated and standardized original IC data $\boldsymbol{X}^*_{IC} = \{\boldsymbol{X}^*_{-m_0+1}, \boldsymbol{X}_{-m_0+2^*}, \ldots, \boldsymbol{X}^*_0\}$ be $(\widehat{\mathbf{m}}^*)^{(0)} = ((\widehat{m}^*_1)^{(0)}, (\widehat{m}^*_2)^{(0)}, \ldots, (\widehat{m}^*_p)^{(0)})'$, the sample medians from the combined IC data up to the previous time point $n-1$ be $(\widehat{m}^*_j)^{(n-1)}$, for $j = 1, 2, \ldots, p$, and the decorrelated and standardized process observations by time $n-1$ that

are immediately before and after $(\widehat{m}_j^*)^{(n-1)}$ be $X_{j,b}^*$ and $X_{j,a}^*$, respectively. Then, the sample median of the jth component by time n, denoted as $(\widehat{m}_j^*)^{(n)}$, is one of $\{X_{j,b}^*, (\widehat{m}_j^*)^{(n-1)}, X_{j,a}^*\}$, depending on whether $(m_0+n-1)/2$ and $(m_0+n)/2$ specify different observations at times $n-1$ and n and which partitioning interval the new decorrelated and standardized observation X_{nj}^* belongs to.

The proposed CUSUM chart for monitoring serially correlated multivariate data with unknown and nonparametric IC process distribution can then be summarized below.

Proposed CUSUM Chart for Monitoring Serially Correlated Multivariate Data

- When $n = 1$, define the standardized observation to be $\boldsymbol{X}_n^* = [\widehat{\gamma}^{(0)}(0)]^{-1/2}(\boldsymbol{X}_n - \widehat{\boldsymbol{\mu}}^{(0)})$. Calculate the charting statistic C_n using (4), in which the vector of sample medians of the decorrelated and standardized IC dataset, $(\widehat{\mathbf{m}}^*)^{(0)}$, is used. The chart gives a signal if (5) is true.

- When $n > 1$, if $T_{n-1} = 0$, then define $\boldsymbol{X}_n^* = [\widehat{\gamma}^{(n-1)}(0)]^{-1/2}(\boldsymbol{X}_n - \widehat{\boldsymbol{\mu}}^{(n-1)})$. Otherwise, the estimated covariance matrix of $(\boldsymbol{X}'_{n-T_{n-1}}, \boldsymbol{X}'_{n-T_{n-1}+1}, \ldots, \boldsymbol{X}'_n)'$ can be defined to be

$$\widehat{\boldsymbol{\Sigma}}_{n,n} = \begin{pmatrix} \widehat{\gamma}^{(n-1)}(0) & \cdots & \widehat{\gamma}^{(n-1)}(T_{n-1}) \\ \vdots & \ddots & \vdots \\ \widehat{\gamma}^{(n-1)}(T_{n-1})^T & \cdots & \widehat{\gamma}^{(n-1)}(0) \end{pmatrix} = \begin{pmatrix} \widehat{\boldsymbol{\Sigma}}_{n-1,n-1} & \widehat{\boldsymbol{\sigma}}_{n-1} \\ \widehat{\boldsymbol{\sigma}}'_{n-1} & \widehat{\gamma}^{(n-1)}(0), \end{pmatrix},$$

  where $\widehat{\boldsymbol{\sigma}}_{n-1} = (\widehat{\gamma}^{(n-1)}(T_{n-1})', \ldots, \widehat{\gamma}^{(n-1)}(1)')'$, and $\widehat{\boldsymbol{\mu}}^{(n-1)}$ and $\widehat{\gamma}^{(n-1)}(s)$, for $s = 0, 1, \ldots, T_{n-1}$, are defined in (1) and (2). Then, the decorrelated and standardized observation at time n is defined to be

$$\boldsymbol{X}_n^* = \widehat{D}_n^{-1/2}\left\{\boldsymbol{X}_n - \widehat{\boldsymbol{\mu}}^{(n-1)} - \widehat{\boldsymbol{\sigma}}'_{n-1}\widehat{\boldsymbol{\Sigma}}_{n-1,n-1}^{-1}\widehat{\boldsymbol{e}}_{n-1}\right\},$$

  where $\widehat{D}_n = \widehat{\gamma}^{(n-1)}(0) - \widehat{\boldsymbol{\sigma}}'_{n-1}\widehat{\boldsymbol{\Sigma}}_{n-1,n-1}^{-1}\widehat{\boldsymbol{\sigma}}_{n-1}$, and $\widehat{\boldsymbol{e}}_{n-1} = ((\boldsymbol{X}_{n-T_{n-1}} - \widehat{\boldsymbol{\mu}}^{(n-1)})', \ldots, (\boldsymbol{X}_{n-1} - \widehat{\boldsymbol{\mu}}^{(n-1)})')'$. Then, we calculate C_n by (4), in which the updated vector of median estimates, $(\widehat{\mathbf{m}}^*)^{(n)} = ((\widehat{m}_1^*)^{(n)}, (\widehat{m}_2^*)^{(n)}, \ldots, (\widehat{m}_p^*)^{(n)})'$, needs to be used. If $C_n = 0$, then define $T_n = 0$. Otherwise, define $T_n = \min(T_{n-1}+1, w)$. The chart gives a signal when (5) is true.

This chart is called G-MCUSUM chart hereafter, where "G" represents "general". To simplify the computation of the above procedure, the following recursive formula should be useful: for $n \geq 2$,

$$\Sigma_{n,n}^{-1} = \begin{pmatrix} \Sigma_{n-1,n-1}^{-1} + \Sigma_{n-1,n-1}^{-1}\boldsymbol{\sigma}_{n-1}D_n^{-1}\boldsymbol{\sigma}'_{n-1}\Sigma_{n-1,n-1}^{-1}, & -\Sigma_{n-1,n-1}^{-1}\boldsymbol{\sigma}_{n-1}D_n^{-1} \\ -D_n^{-1}\boldsymbol{\sigma}'_{n-1}\Sigma_{n-1,n-1}^{-1}, & D_n^{-1} \end{pmatrix}.$$

To compute $\widehat{\Sigma}_{n,n}^{-1}$ by the above recursive formula, we can replace the related quantities on the right-hand-side by their estimates.

In the CUSUM chart (4)-(5), the allowance constant k is usually pre-specified together with the IC average run length ARL_0. Given the values of k and ARL_0, h can be computed from the IC dataset by a bootstrap resampling approach (cf., Chatterjee and Qiu 2009). Because the process observations at diferent time points could be serially correlated, we suggest using a block bootstrap procedure (cf., Lahiri 2003) that is described below. The categorized IC data after data decorrelation and standardization are denoted as $\{\boldsymbol{Y}_t, t = -m_0+1, ..., 0\}$. Then, the block bootstrap procedure with the block size of l consists of the following several steps:

Step 1: There are a total of m_0-l+1 possible blocks of length l. The kth block is $\{\boldsymbol{Y}_{-m_0+k+i}, 0 \le i \le l-1\}$, for $k = 1, 2, \ldots, m_0 - l + 1$. Randomly select a sequence of integers with replacement from the set $\{1, 2, \ldots, m_0 - l + 1\}$. Then, the corresponding blocks of IC data are put one after another according to the selection order, to form a bootatrap sample of IC data.

Step 2: For a given control limit h, apply the CUSUM chart (4)-(5) to the bootstrap sample obtained in Step 1. The run length is defined as $RL_0(h) = \min\{i : C_i > h\}$.

Step 3: Repeat Steps 1 and 2 for B times, and define $ARL_0(h)$ to be the sample average of the B values of $RL_0(h)$ obtained from the B replicated simulations.

Step 4: Use the bisection search algorithm to search for the value of h such that $ARL_0(h)$ reaches the pre-specified value of ARL_0 (cf., Qiu 2008).

In all simulation examples in Section 3, we use $B = 1,000$ in the block bootstrap procedure. Also, based on an extensive numerical study, the block size l can be chosen between 40 and 50. The performance of the proposed chart G-MCUSUM is reasonably good when l is chosen in that range under various serial data correlation structure. So, we choose $l = 50$ in Section 3. When describing serial data correlation, it has been assumed that the correlation between two process observations can be ignored if their observation times are at least $w + 1$ points apart. In applications, w is often unknown and it needs to be pre-specified beforehand in order to use the proposed method. Of course, selection of w is usually application-specific. Theoretically, w should be chosen large to avoid mis-specification of the serial data correlation. But, the estimates of $\{\boldsymbol{\gamma}(s), 0 \le s \le w\}$ may not be reliable when w is chosen too large, especially in the initial period of process monitoring, because of their large variability. Based on our numerical experience, our proposed method should perform reasonably well under a wide range of serial data correlation structures if we choose w in the range $[15, 25]$. In all simulation examples in Section 3, we choose $w = 20$.

3 Numerical Studies

We present some simulation results in this section about the performance of the proposed control chart G-MCUSUM. For comparison purposes, the following five alternative methods are also considered. They should represent the state-of-the-art nonparametric MSPC charts in the literature well.

- Nonparameteric multivariate CUSUM control chart suggested in Qiu (2008), denoted as NP-MCUSUM. This chart is based on data categorization and it is a distribution-free chart. But, it cannot accommodate serial data correlation. Its IC parameters are estimated from the IC data, but the estimates are not updated recursively during online process monitoring. Thus, it is not a self-starting chart.

- Cumulative sum of T chart that was suggested by Crosier (1988), denoted as COT. This method applies the conventional upward CUSUM chart to the sequence $\{T_n, n \geq 1\}$, where $T_n^2 = (\boldsymbol{X}_n - \widehat{\boldsymbol{\mu}}^{(0)})'[\widehat{\boldsymbol{\gamma}}^{(0)}(0)]^{-1}(\boldsymbol{X}_n - \widehat{\boldsymbol{\mu}}^{(0)})$ is the Hotelling's chi-square statistic.

- A modified version of COT, denoted as SC-COT, which is the same as COT, except that data decorelation is applied to each quality variable separately and different quality variables are assumed independent.

- The multivariate control chart discussed in Kalgonda and Kulkarni (2004), denoted as Z. This chart was designed for detecting mean shifts of serially correlated multivariate processes. At the current time point n, the charting statistic of Z is defined as $Z_n = \max_{1\leq j\leq p}|Z_{nj}|$, where $Z_{nj} = (X_{nj} - \widehat{\mu}_j^{(0)})/\sqrt{\widehat{\gamma}_{jj}^{(0)}(0)}$, for $j = 1, 2, \ldots, p$ and $n \geq 1$, where $\widehat{\mu}_j^{(0)}$ is the jth element of $\widehat{\boldsymbol{\mu}}^{(0)}$ and $\widehat{\gamma}_{jj}^{(0)}(0)$ is the (j,j)th element of $\widehat{\boldsymbol{\gamma}}^{(0)}(0)$.

- A simplified version of the chart G-MCUSUM, denoted as G1-MCUSUM, which is the same as G-MCUSUM, expect that estimates of all IC parameters from the IC data are not updated recursively during online process monitoring.

In the simulation studies, the following four IC models are considered. Without loss of generality, in all cases considered, we set the number of quality variables to be $p = 3$.

Case I Process observations $\{\boldsymbol{X}_1, \boldsymbol{X}_2, \ldots\}$ are i.i.d. with the IC distribution $N_3(\boldsymbol{0}, I_{3\times 3})$, where $I_{3\times 3}$ is the 3×3 identity matrix.

Case II Process observations $\{\boldsymbol{X}_n = (X_{n1}, X_{n2}, X_{n3})', n \geq 1\}$ are generated as follows. X_{n1} follows the AR(1) model $X_{n1} = 0.1X_{n-1,1} + \varepsilon_n$, for $n \geq 1$, where $X_{01} = 0$ and $\{\varepsilon_n\}$ are

i.i.d. random errors with the $N(0, 0.1^2)$ distribution. X_{n2} and X_{n1} are associated, and $X_{n2} = X_{n1} + 0.1\xi$, where ξ is a standardized version of a random variable from the distribution χ^2_3 and ξ is independent of $\{X_{n1}\}$. X_{n3} and X_{n1} are independent, and X_{n3} follows the AR(1) model $X_{n3} = 0.2X_{n-1,3} + \varepsilon_n$, for $n \geq 1$, where $X_{03} = 0$ and $\{\varepsilon_n\}$ are i.i.d. random errors with the $N(0, 0.1^2)$ distribution.

Case III Process observations $\{\boldsymbol{X}_n = (X_{n1}, X_{n2}, X_{n3})', n \geq 1\}$ are generated as follows. X_{n1} follows the AR(1) model $X_{n1} = 0.5X_{n-1,1} + \varepsilon_n$, for $n \geq 1$, where $X_{01} = 0$ and $\{\varepsilon_n\}$ are i.i.d. random errors with the $N(0, 0.1^2)$ distribution. X_{n2} and X_{n1} are associated, and $X_{n2} = X_{n1} + 0.1\xi$, where ξ is a standardized version of a random variable from the distribution χ^2_3 and ξ is independent of $\{X_{n1}\}$. X_{n3} and X_{n1} are independent, and X_{n3} follows the AR(1) model $X_{n3} = -0.5X_{n-1,3} + \varepsilon_n$, for $n \geq 1$, where $X_{03} = 0$ and $\{\varepsilon_n\}$ are i.i.d. random errors with the $N(0, 0.1^2)$ distribution.

Case IV Process observations follow the model $\boldsymbol{X}_n = (1, 2, 1)' + A\boldsymbol{X}_{n-1} + \boldsymbol{\varepsilon}_n$, for $n \geq 2$, where $\{\boldsymbol{\varepsilon}_n\}$ are i.i.d. with the $N_3(\mathbf{0}, B)$ distribution, where

$$A = \begin{bmatrix} 0.5 & 0 & 0 \\ 0 & 0.7 & 0 \\ 0 & 0 & 0.2 \end{bmatrix}, \qquad B = \begin{bmatrix} 1 & 0.2 & 0.2 \\ 0.2 & 1 & 0.2 \\ 0.2 & 0.2 & 1 \end{bmatrix}.$$

Case I described above is the conventional situation considered in the MSPC literature that multivariate process observations are i.i.d. with a normal IC distribution. Cases II and III consider the scenarios when process observations are serially correlated and two quality variables (i.e., X_{n1} and X_{n2}) are associated as well. The main difference between Cases II and III is that the serial data correlation is stronger in Case III than that in Case II. Case IV considers a scenario when all quality variables are serially correlated and associated with each other as well.

3.1 IC performance

We first evaluate the IC performance of the related control charts. In the simulation study, the IC sample size m_0 is first fixed at 500, and the nominal ARL_0 value is fixed at 200 in each control chart. In the three CUSUM charts G-MCUSUM, G1-MCUSUM, NP-CUSUM, the allowance constants are all chosen to be 0.01. In the COT and SC-COT charts, the allowance constants are both chosen to be 1.5, as suggested by Crosier (1988) for the COT chart. The control limits of the charts G-MCUSUM and G1-MCUSUM are both computed by the block bootstrap procedure described at the end of Section 2 with the block size of 50. The control limits of the other four

charts NP-CUSUM, COT, SC-COT and Z are computed as discussed in the papers Qiu (2008), Crosier (1988) and Kalgonda and Kulkarni (2004). The actual ARL_0 value of a control chart is computed as follows. First, an IC data of size m_0 is generated. Then, the control chart is applied to a sequence of 2,000 process observations for online process monitoring, and the run length (RL) value is recorded. This step is repeated for 1,000 times and the average of the 1,000 RL values is calculated as an estimate of the ARL_0 value. Then, the entire simulation, from generation of the IC data to calculation of the ARL_0 estimate, is repeated for 100 times. The average of the 100 ARL_0 estimates is used as the calculated actual ARL_0 value. The standard error of the calculated actual ARL_0 value can also be calculated. The calculated actual ARL_0 values of the six control charts are presented in Table 1, along with their standard errors (in parentheses). From the table, it can be seen that (i) G1-MCUSUM, NP-CUSUM, COT, SC-COT and Z do not perform well in most cases considered, and (ii) G-MCUSUM is reliable to use in all cases considered. The explanations for the result (i) are that 1) all the five alternative charts G1-MCUSUM, NP-CUSUM, COT, SC-COT and Z are not self-starting and their performance would be affected by relatively poor accuracy of the IC parameter estimates obtained from the IC data, and 2) they cannot accommodate data correlation well. As a comparison, the proposed chart G-MCUSUM overcomes both of these two limitations.

Table 1: Actual ARL_0 values and their standard errors (in parentheses) of six control charts when their nominal ARL_0 values are fixed at 200 and the IC sample size m_0 is fixed 500.

	G-MCUSUM	G1-MCUSUM	NP-CUSUM	COT	SC-COT	Z
Case I	204 (4.06)	130 (2.98)	124 (2.89)	216 (4.46)	185 (4.06)	255 (5.01)
Case II	196 (3.49)	105 (2.09)	68 (1.99)	218 (3.40)	189 (4.21)	274 (5.41)
Case III	195 (4.16)	104 (2.15)	42 (1.46)	166 (3.08)	267 (5.62)	296 (5.01)
Case IV	195 (3.52)	114 (2.67)	37 (1.61)	173 (3.20)	289 (5.85)	247 (4.80)

The performance of the proposed chart G-MCUSUM could depend on the IC sample size m_0. To see how m_0 affects the performance of G-MCUSUM, we let m_0 change among 200, 300, 400, 500 and 1000, and the remaining setup is kept unchanged from those in the example of Table 1. The calculated actual ARL_0 values of G-MCUSUM are presented in Table 2. From the table, it can be seen that the IC performance of G-MCUSUM when $m_0 = 200$ or 300 is not quite reliable because the differences between the actual and nominal ARL_0 values are more than 10% of the nominal ARL_0 value in Cases I-IV. When m_0 gets larger, the IC performance of G-MCUSUM gets more reliable. Its IC performance is reliable in this example when $m_0 \geq 500$. Of course, the necessary IC sample size would depend on the dimensionality of the process under monitoring. When the dimension p gets larger, the necessary value of m_0 should be larger as well. To see this, we perform

a small simulation study after modifying Case IV into Case IV* below.

Case IV* Assume that observations of a 10-dimensional process follow the model

$$\boldsymbol{X}_n = (1,2,1,1,2,1,1,2,1,1)' + A^*\boldsymbol{X}_{n-1} + \boldsymbol{\varepsilon}_n, \text{ for } n \geq 2,$$

where $\{\boldsymbol{\varepsilon}_n\}$ are i.i.d. with the $N_{10}(\mathbf{0}, B^*)$ distribution, A^* is a diagonal matrix with the diagonal elements being 0.5, 0.7, 0.2, 0.5, 0.7, 0.2, 0.5, 0.7, 0.2, 0.5, and B^* is a 10×10 covariance matrix with all diagonal elements being 1 and all off-diagonal elements being 0.2.

In Case IV*, when m_0 changes among 500, 1000, 2000 and 3000 and other setups are the same as those in the example of Table 2, the actual ARL_0 values and their standard errors are presented in Table 3. From the table, it can be seen that the necessary IC sample size should be 2000 or larger in this example when $p = 10$.

Table 2: Actual ARL_0 values and their standard errors (in parentheses) of G-MCUSUM when its nominal ARL_0 value is fixed at 200, $p = 3$, and the IC sample size m_0 changes among 200, 300, 400, 500 and 1000.

	$m_0 = 200$	300	400	500	1000
Case I	283 (7.46)	269 (6.89)	238 (6.14)	204 (4.06)	202 (3.90)
Case II	250 (6.31)	236 (5.93)	220 (5.34)	196 (3.49)	198 (3.58)
Case III	271 (6.75)	230 (5.87)	214 (4.91)	195 (4.16)	199 (3.98)
Case IV	236 (6.04)	224 (5.67)	212 (4.67)	195 (3.52)	198 (3.62)

Table 3: Actual ARL_0 values and their standard errors (in parentheses) of G-MCUSUM when its nominal ARL_0 values are fixed at 200, $p = 10$, and the IC sample size m_0 changes among 500, 1000, 2000 and 3000.

	$m_0 = 500$	1000	2000	3000
Case IV*	327 (7.65)	242 (5.87)	218 (4.96)	202 (3.76)

3.2 OC performance

Next, we study the OC performance of the related control charts in cases when $p = 3$, $m_0 = 500$ and $ARL_0 = 200$. To make the comparison meaningful, we intentionally adjust the control limits of the charts G1-MCUSUM, NP-MCUSUM, COT, SC-COT and Z so that their actual ARL_0 values equal 200 in all cases considered. In the simulation study, we assume that a shift in each component

of $\boldsymbol{X}_n$ occurs at the beginning of Phase II monitoring. In cases I, II and III, the shift size is $\delta\sigma_X$, where σ_X is the IC standard deviation of the specific component and δ changes from -1.0 to 1.0 with a step of 0.25. In case IV, the shift size is δ that changes from -1.0 to 1.0 with a step of 0.25. Because different control charts have different procedure parameters (i.e., the allowance constant of the five multivariate CUSUM-type charts) and their performance may not be comparable if their parameters are set to be the same, we choose the allowance constant of each of G-MCUSUM, G1-MCUSUM, NP-MCUSUM, COT and SC-COT so that its calculated ARL_1 value reaches the minimum for detecting a specific shift. Namely, we compare their optimal OC performance in this part. Because the chart Z is a Shewhart chart, it does not have such a procedure parameter to choose. The actual ARL_1 values are computed in the same way as that for computing ARL_0, except that the Phase II process observations have a mean shift at the beginning of online process monitoring. The calculated ARL_1 values of the six charts in various cases are shown in Figure 1. From the plots in the figure, it can be seen that i) the proposed method G-MCUSUM performs the best in almost all cases considered, ii) G1-MCUSUM performs slightly better than G-MCUSUM in cases when the shift is small, but its performance becomes worse when the shift gets larger, and iii) the other four charts NP-MCUSUM, COT, SC-COT and Z do not perform well in all cases considered. The conclusions i) and iii) are intuitively reasonable because a) the alternative charts NP-MCUSUM, COT, SC-COT and Z cannot accommodate data correlation properly and their performance would be affected by the IC data size since some of their IC parameters need to be estimated from the IC data, and b) the proposed chart G-MCUSUM can accommodate data correlation and its dependence on the IC data size is smaller since it is a self-starting chart. The conclusion ii) can be explained by the fact that the self-starting chart G-MCUSUM could miss some shifts, especially when the shifts are small. See a related discussion in Section 4.5 of Qiu (2014). In addition, it has been well demonstrated in the literature that data decorrelation could attenuate the shift effect and make the related control chart less sensitive to a shift (Apley and Tsung 2002). This is the so-called "masking" effect. You and Qiu (2019) showed that such a "masking" effect can be reduced by using the spring length T_n in data decorrelation (cf., the related discussion after Expression (2) in Section 2), since T_n is often a small integer number and thus only a small number of previous process observations are involved in the data decorrelation at the current time point n. Results in Figure 1 have partly confirmed this conclusion, since G-MCUSUM outperforms NP-MCUSUM in all cases considered and the latter did not consider data decorrelation.

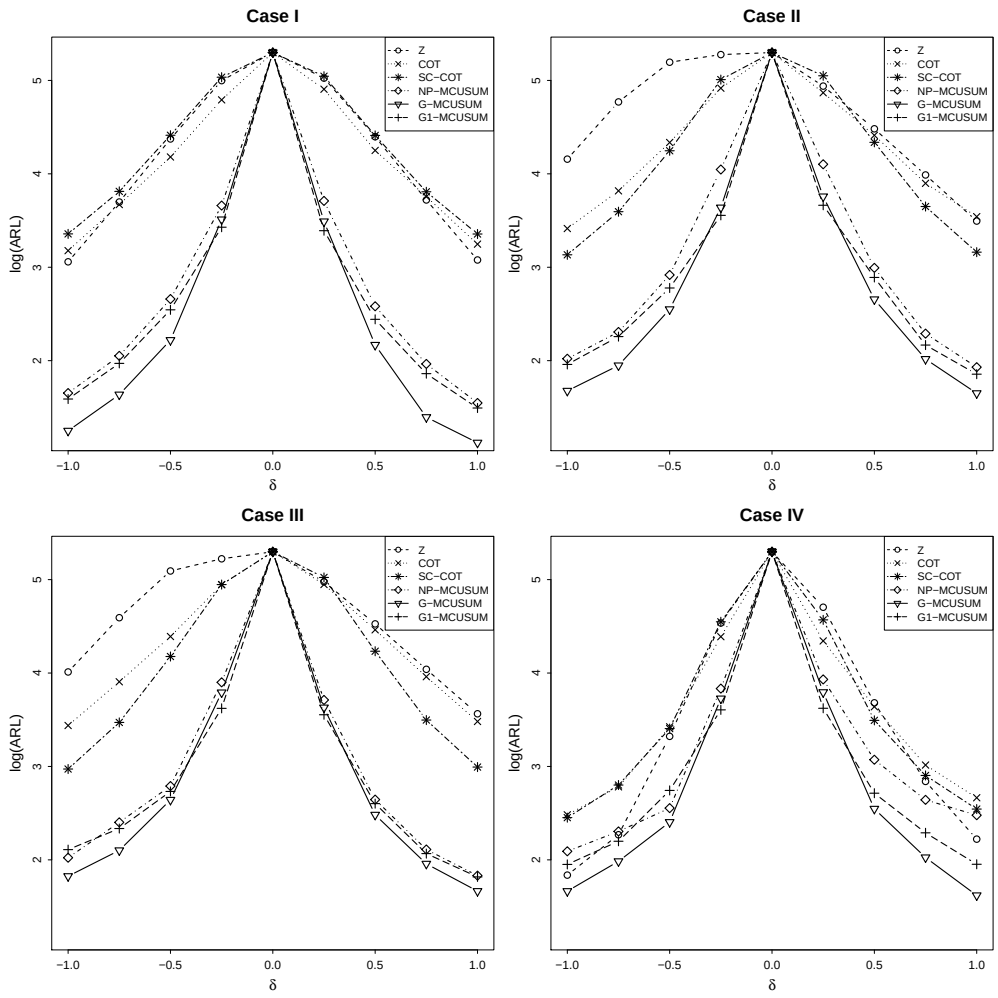

Figure 1: Calculated optimal ARL_1 values of the six control charts when $p = 3$, $ARL_0 = 200$, $m_0 = 500$, and the procedure parameters are chosen in the way such that the calculated ARL_1 values reach the minimum for detecting a given shift.

The OC performance of the chart G-MCUSUM could be affected by the IC data size m_0. In the next example, we let m_0 change among 200, 500, 1,000 and 2,000, and other chart setups remain the same as those in the example of Figure 1. The calculated optimal ARL_1 values of the chart are shown in Figure 2. From the plots, it can be seen that i) the larger the value of m_0, the better the performamce of G-MCUSUM, ii) the chart's performance is quite stable in most cases when $m_0 \geq 500$, and iii) the chart's performance is reasonably stable in all cases considered when $m_0 \geq 1,000$.

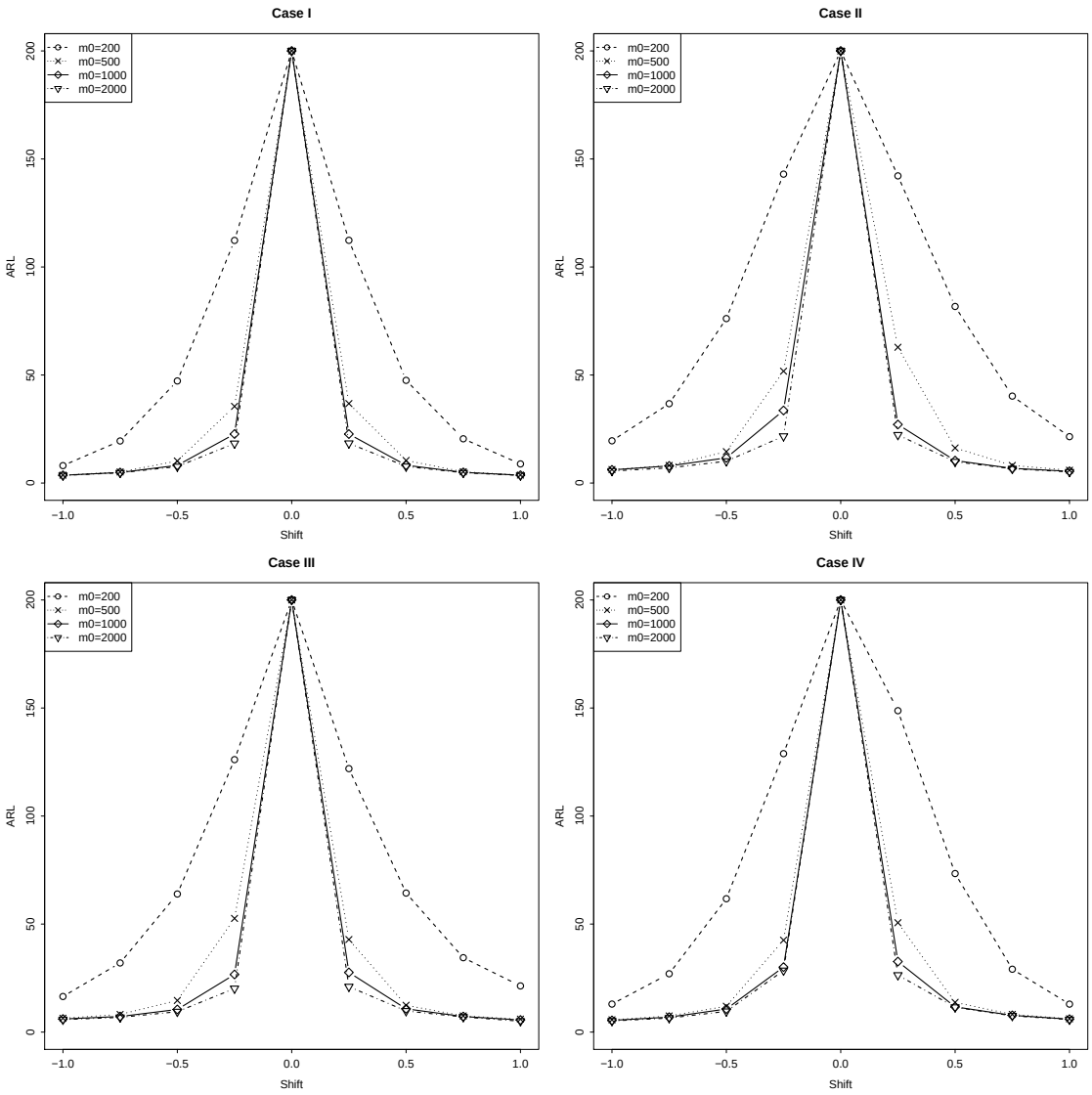

Figure 2: Calculated optimal ARL_1 values of the chart G-MCUSUM when $ARL_0 = 200$, $m_0 = 200, 500, 1000$ or 2000, and the allowance constant is chosen such that the calculated ARL_1 value reaches the minimum for detecting a given shift.

In the next example, we study the impact of k on the performance of G-MCUSUM by changing the k value among $\{0.001, 0.005, 0.01, 0.05, 0.1\}$ and keeping the other chart setups the same as those in the example of Figure 1. The calculated ARL_1 values of the chart G-MCUSUM are shown in Figure 3. From the plots, we can see that the OC performance of G-MCUSUM is quite stable in all cases considered when $k \leq 0.01$, and a small k value (e.g., 0.001) is good for detecting small shifts (e.g., the shifts ± 0.25 in Case II).

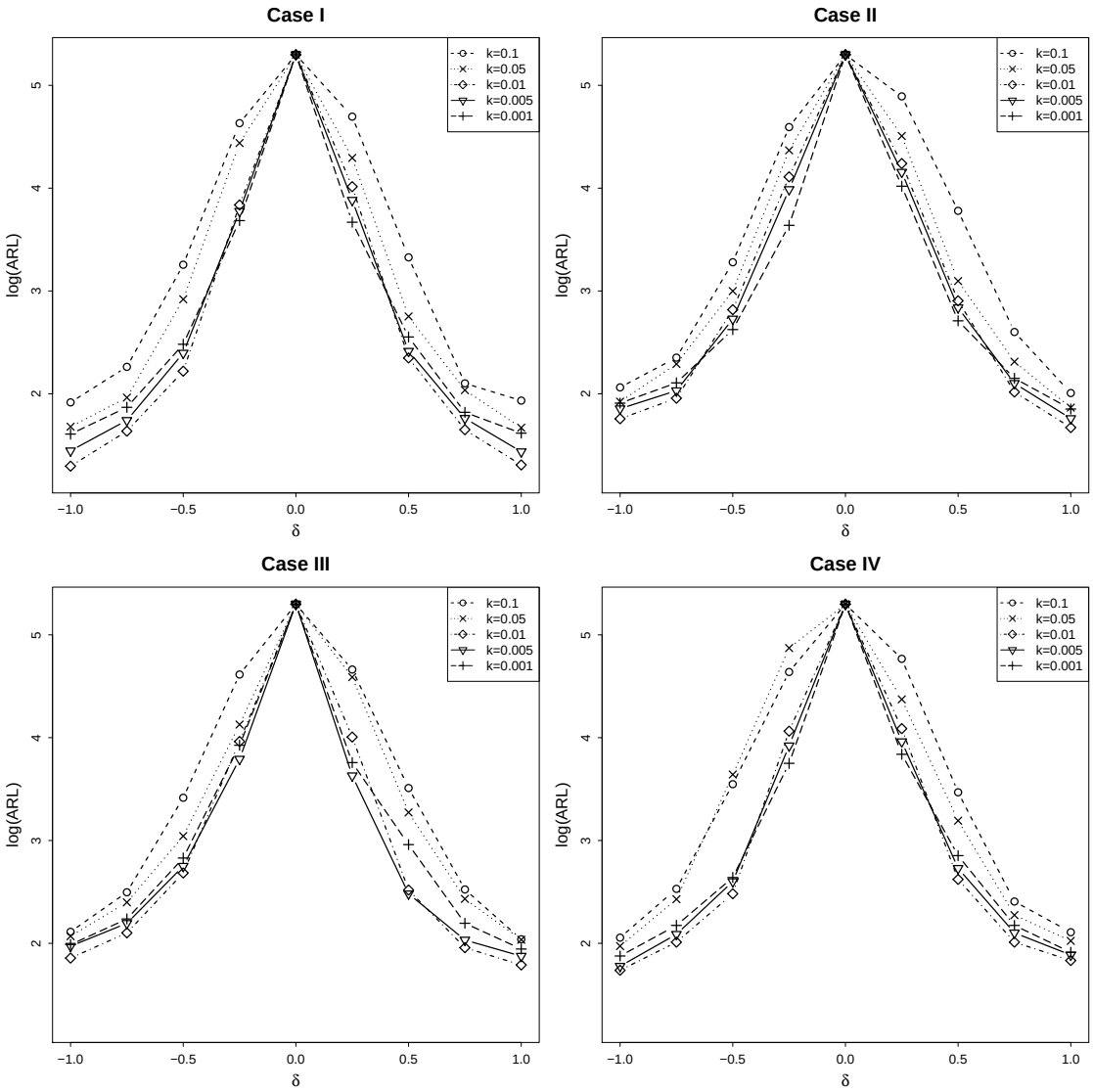

Figure 3: Calculated ARL_1 values of the chart G-MCUSUM when $ARL_0 = 200$, $m_0 = 500$, and k changes among $\{0.001, 0.005, 0.01, 0.05, 0.1\}$.

4 A Real Data Example

In this section, we illustrate the proposed control chart using a real-data example about the semiconductor manufacturing process data that are maintained by the University of California, Irvine Machine Learning Repository. The dataset was collected from July 2008 to October 2008 by a computerized system that automatically manages the semiconductor manufacturing process. The process consists of a series of sequential process steps in which layers of materials are deposited on substrates, doped with impurities, and patterned using photolithography to produce sophisti-

cated integrated circuits and devices. The key quality variables for each step are under constant surveillance by the monitoring of data streams collected from sensors at many key measurement points (May and Spanos 2006). The variables may characterize physical parameters, such as film thickness and uniformity, or electrical parameters, such as resistance and capacitance. The data used in this section consist of 500 observations of three quality variables, denoted as V1, V2 and V3. The data are shown in Figure 4. From the plots in the figure, it can be seen that the first 400 observations are quite stable over time. Thus, they are used as the IC data. For the IC data, the Shapiro test for checking the normality assumption gives a p-value of 2.2×10^{-16}, which implies that the distribution of the IC data is significantly different from a normal distribution. Then, we use the Durbin-Watson test for checking data autocorrelation in each quality variable. The test gives p-values of $0.112, 1.297 \times 10^{-5}, 3.178 \times 10^{-3}$, respectively, for the three variables. Thus, there is a significant autocorrelation in the IC data for the second and third quality variables. The sample correlation matrix of the IC data is computed to be

$$\begin{pmatrix} 1 & -0.041 & -0.065 \\ -0.041 & 1 & 0.144 \\ -0.065 & 0.144 & 1 \end{pmatrix}.$$

The t-tests for checking whether the Pearson's correlation correlations between quality variables in the three pairs (V1,V2), (V1,V3) and (V2,V3) are 0 give p-values of 0.4154, 0.1930 and 0.0038, respectively. Thus, there is a significant correlation between V2 and V3 in the IC data.

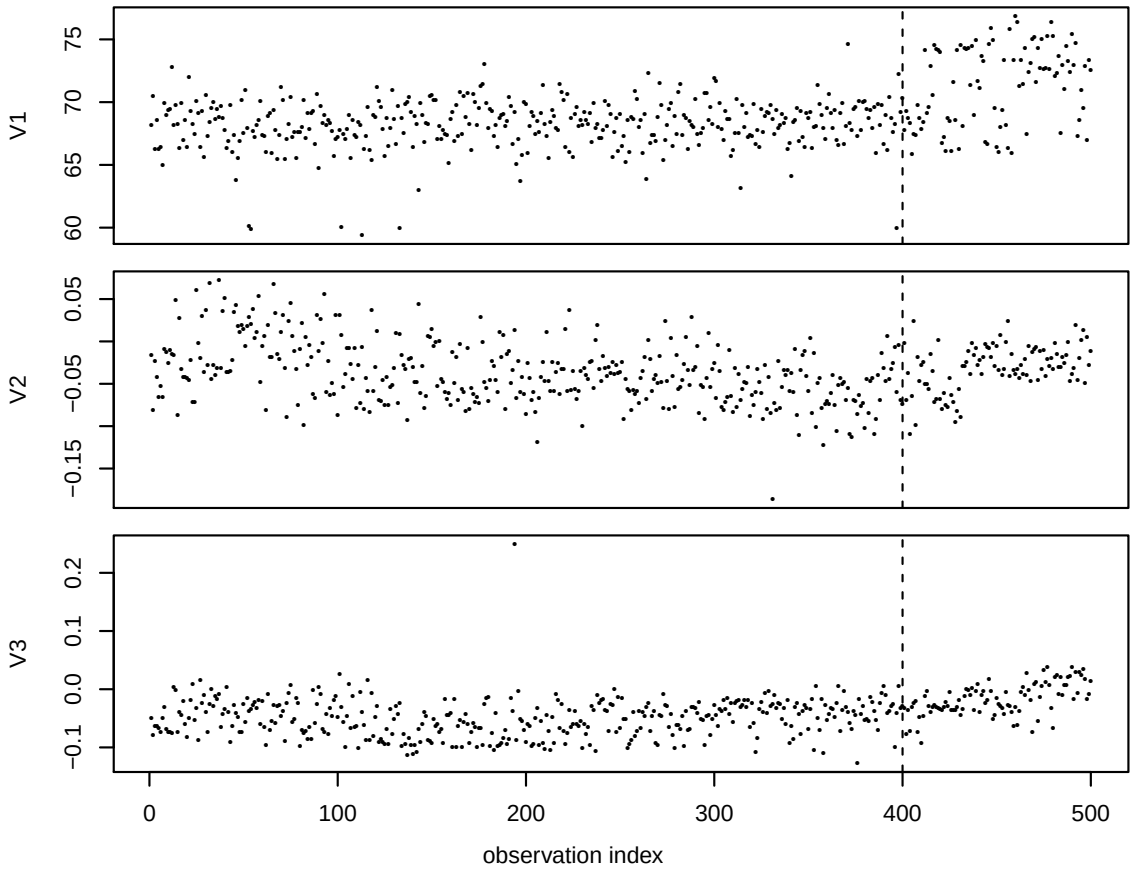

Figure 4: Original observations of the semiconductor manufacturing process data. The vertical dashed line in each plot separates the IC data from the Phase II process observations.

For this data, the charts NP-CUSUM, COT, SC-COT and Z may not be appropriate to use, since they cannot accommodate data autocorrelation and the charts COT and Z require the normality assumption as well. As a comparison, the charts G-MCUSUM and G1-MCUSUM should be appropriate to use, and the chart G-MCUSUM might have some advantages to detect relatively large shifts, in comparison with G1-MCUSUM, since the former is a self-starting chart. Now, we try to apply the six charts G-MCUSUM, G1-MCUSUM, NP-CUSUM, COT, SC-COT and Z to this dataset for monitoring its last 100 observations. In all charts, we set $ARL_0 = 200$. Their control limits are computed in the same way as that in the simulation studies presented in Section 3. The allowance constant k in the three CUSUM charts G-MCUSUM, G1-MCUSUM, NP-CUSUM is chosen to be 0.01, and the allowance constant k in the charts COT and SC-COT is chosen to be 1.5, as suggested by Crosier (1988) for the COT chart. The six charts for monitoring the last 100 observations of the dataset are shown in Figure 5, where the dashed horizontal lines denote

their control limits. From the plots, we can see that the charts G-MCUSUM, G1-MCUSUM, NP-CUSUM, COT, SC-COT and Z give their first signals at the 23th, 26th, 26th, 31st, 65th and 62th Phase II observation times, respectively. Therefore, the first signal by G-MCUSUM is the earliest in this example, and the first signals by the other five charts are 3, 3, 8, 42 and 39 days later. This example confirms that the proposed chart G-MCUSUM is effective in detecting distributional shifts in this semiconductor manufacturing process data.

5 Concluding Remarks

MSPC is an important research problem since most processes for quality monitoring in practice would concern multiple quality variables. In the literature, almost all existing MSPC methods assume that process observations at different time points are independent, which is rarely valid in practice. In the previous sections of this paper, we have described a new MSPC method that can accommodate serial data correlation properly. It is a self-starting nonparametric chart, in the sense that it is robust to the IC process distribution and does not require a large IC dataset to set up its design. These features make it an ideal tool for MSPC applications. Numerical studies presented in Sections 3 and 4 show that it performs well in different cases considered. This chart is based on two mild assumptions. One is that the IC serial data correlation is startionary, and the other one is that the correlation between two process observations becomes weaker and weaker when the two observation times get farther apart. These two assumptions should be valid (at least asymptotically) in most applications. But, there could be some processes in practice with long-range data dependence (cf., Beran 1992). Some new MSPC methods are needed for handling such applications. The proposed method is based on recursive data decorrelation and standardization and on recursive update of the IC parameter estimates as well. The recursive nature makes the computation relatively easy. But, in cases when the number of quality variables is very large, the computing burden might become substantial. In such cases, some variable selection approaches might be helpful (cf., Wang and Jiang 2009, Zou and Qiu 2009), which will be further explored in our future research.

Acknowledgements

We would like to thank the editor and a referee for some constructive comments and suggestions, which improved the quality of the paper greatly. Peihua Qiu's research was supported in part by the NSF grant DMS-1914639 in USA. Li Xue's research was supported in part by the grants

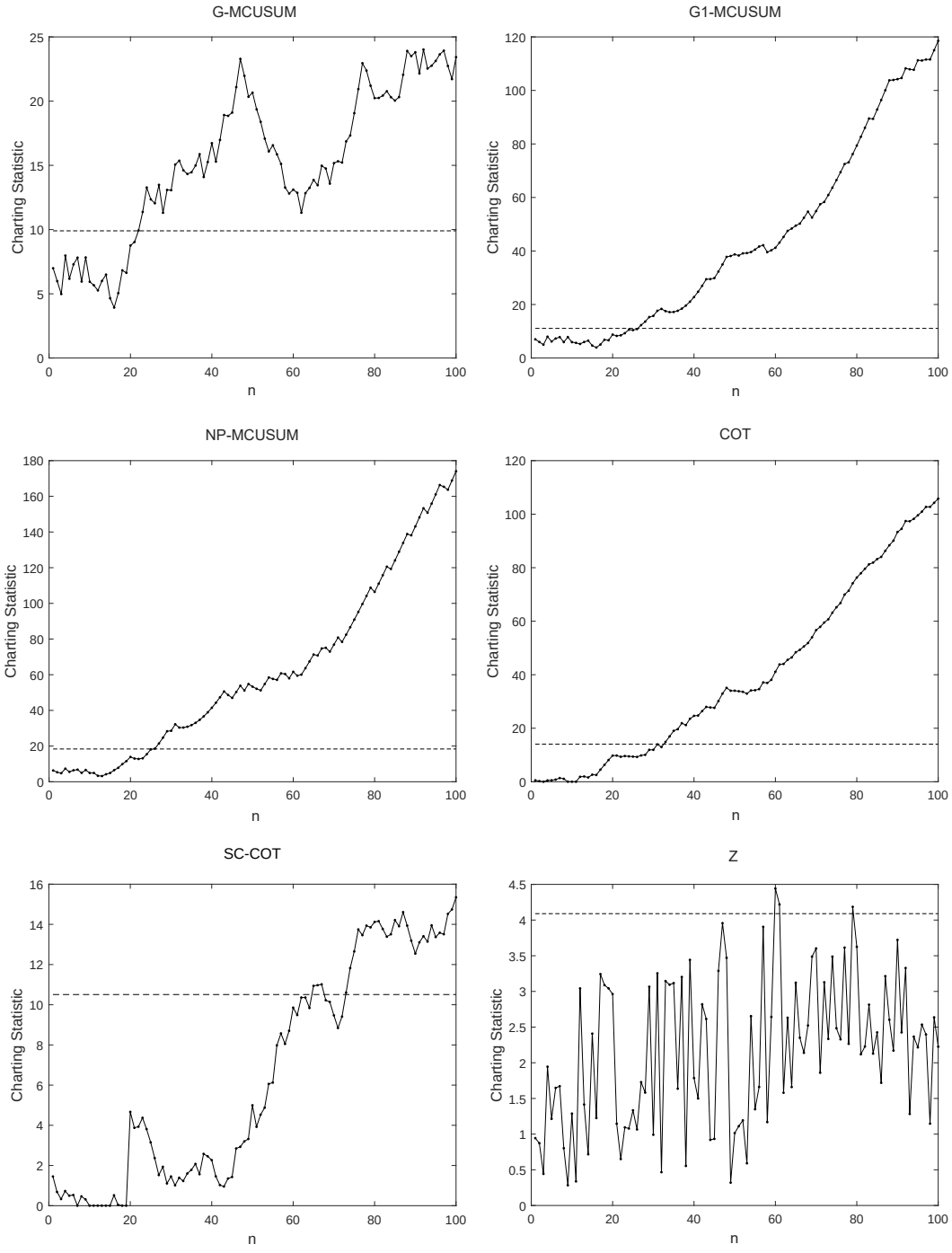

Figure 5: Control charts G-MCUSUM, G1-MCUSUM, NP-MCUSUM, COT, SC-COT and Z when they are applied to the Phase II semiconductor manufacturing process data shown in Figure 4. The horizontal dashed line in each plot is the control limit of the related control chart.

71701188, 71672209 and 71871204 from the National Natural Science Foundation of China, the grant 2016M601266 from the China Postdoctoral Science Foundation, the grant 19HASTIT032 from the Science and Technology Innovation Talent Support plan in Universities of Henan Province of China, and the grant 2016GGJS-112 from the Training Program for Young Key Teachers in Universities of Henan Province.

References

Agresti, A. (2013), *Categorical Data Analysis (3rd edition)*, John Wiley & Sons: New York.

Apley D.W., and Lee, H.C. (2008), "Robustness comparison of exponentially weighted moving-average charts on autocorrelated data and on residuals," *Journal of Quality Technology*, **40**, 428–447.

Apley D.W., and Tsung, F. (2002), "The autoregressive T^2 chart for monitoring univariate autocorrelated processes," *Journal of Quality Technology*, **34**, 80–96.

Beran, J. (1992), "Statistical methods for data with long-range dependence," *Statistical Science*, **4**, 404-416.

Boone, J.M., and Chakraborti, S. (2012), "Two simple Shewhart-type multivariate nonparametric control charts," *Applied Stochastic Models in Business and Industry*, **28**, 130–140.

Chatterjee, S. and Qiu, P. (2009), "Distribution-free cumulative sum control charts using bootstrap-based control limits," *Annals of Applied Statistics*, **3**, 349–369.

Chen, N., Zi, X., and Zou, C. (2016), "A distribution-free multivariate control chart," *Technometrics*, **58**, 448–459.

Crosier, R B. (1998), "Multivariate generalizations of cumulative sum quality-control schemes," *Technometrics*, **30**, 291–303.

Hawkins, D.M. (1987), "Self-starting cusums for location and scale," *The Statistician*, **36**, 299–315.

Hawkins, D.M. (1991), "Multivariate quality control based on regression-adjusted variables," *Technometrics*, **33**, 61–75.

Hawkins, D.M., and Olwell, D.H. (1998), *Cumulative Sum Charts and Charting for Quality Improvement*, New York: Springer-Verlag.

Healy, J.D. (1987), "A note on multivariate CUSUM procedure," *Technometrics*, **29**, 409–412.

Holland, M.D., and Hawkins, D.M. (2014), "A control chart based on a nonparametric multivariate change-point model," *Journal of Quality Technology*, **46**, 63–77.

Kalgonda, A.A., and Kulkarni, S.R. (2004), "Multivariate quality control chart for autocorrelated processes," *Journal of Applied Statistics*, **31**, 317–327.

Lahiri, S.N. (2003), *Resampling Methods for Dependent Data*, New York: Springer.

Li, J., and Qiu, P. (2016), "Nonparametric dynamic screening system for monitoring correlated longitudinal data," *IIE Transactions*, **48**, 772–786.

Li, W., and Qiu, P. (2020), "A general charting scheme for monitoring serially correlated data with short-memory dependence and nonparametric distributions," *IISE Transactions*, **52**, 61–74.

Liu, R.Y. (1995), "Control charts for multivariate processes," *Journal of the American StatisticalAssociation*, **90**, 1380–1387.

Lowry, C.A., Woodall, W.H., Champ, C.W., and Rigdon, S.E. (1992), "Multivariate exponentially weighted moving average control chart," *Technometrics*, **34**, 46–53.

May,G.,and Spanos,C.(2006),*Fundamentals of Semiconduct or Manufacturing and Process Control*, Hoboken,NJ:Wiley.

Montgomery, D.C. (2012), *Introduction to Statistical Quality Control*, New York: John Wiley & Sons.

Qiu, P. (2008), "Distribution-free multivariate process control based on Log-liner modeling, *IIE Transactions*, **40**, 664–677.

Qiu, P. (2014), *Introduction to Statistical Process Control*, Boca Raton, FL: Chapman Hall/CRC.

Qiu, P. (2018), "Some perspectives on nonparametric statistical process control," *Journal of Quality Technology*, **50**, 49–65.

Qiu, P. (2020), "Big data? statistical process control can help!," *The American Statistician*, in press, DOI: 10.1080/00031305.2019.1700163.

Qiu, P., and Hawkins, D.M. (2001), "A rank based multivariate CUSUM procedure," *Technometrics*, **43**, 120–132.

Qiu, P., and Hawkins, D.M. (2003), "A nonparametric multivariate CUSUM procedure for detecting shifts in all directions," *JRSS-D (The Statistician)*, **52**, 151–164.

Qiu, P., Li, W., and Li, J. (2020), "A new process control chart for monitoring short-range serially correlated data," *Technometrics*, **62**, 71–83.

Runger, G. (2002), "Assignable causes and autocorrelation: control charts for observations or residuals?" *Journal of Quality Technology*, **34**, 165–170.

Tracy, N.D., Young, J.C., and Mason, R.L. (1992), "Multivariate control charts for individual observations," *Journal of Quality Technology*, **24**, 88–95.

Wang, K., and Jiang, W. (2009), "High-dimensional process monitoring and fault isolation via variable selection," *Journal of Quality Technology*, **41**, 247–258.

You, L., and Qiu, P. (2019), "Fast computing for dynamic screening systems when analyzing correlated data," *Journal of Statistical Computation and Simulation*, **89**, 379–394.

Zou, C., and Qiu, P. (2009), "Multivariate statistical process control using LASSO," *Journal of American Statistical Association*, **104**, 1586–1596.

Zou, C., and Tsung, F. (2011), "A multivariate sign EWMA control chart," *Technometrics*, **53**, 84–97.

Zou, C., Wang, Z., and Tsung, F. (2012), "A spatial rank-based multivariate EWMA control chart," *Naval Research Logistics*, **59**, 91–110.